

A theoretical and experimental investigation of Raman scattering in the size-quantizing heterostructure superlattices $(\text{GaAs})_m(\text{AlAs})_n$

B. Kh. Bairamov, T. Gant,¹⁾ M. Delaney,¹⁾ Yu. É. Kitaev, M. V. Klein,¹⁾ D. Levi,¹⁾ H. Morkoç,¹⁾ and R. A. Évarestov

A. F. Ioffe Physico-Technical Institute, USSR Academy of Sciences

(Submitted 10 November 1988)

Zh. Eksp. Teor. Fiz. **95**, 2200–2210 (June 1989)

We report the experimental observation of first- and second-order Raman scattering in the semiconductor superlattices $(\text{GaAs})_m(\text{AlAs})_n$ under optical excitation far from resonance with the exciton transition. We show that for various combinations of the numbers of monolayers m and n there exist only eight inequivalent ways to distribute the atoms on the basis of Wyckoff positions. In order to analyze the symmetries of the phonons we have used the method of band representations of the space groups. We have determined the selection rules for the second-order Raman spectra and have interpreted the results of our experiments in terms of them. We establish that the contribution the displacement of a specific atom makes to the phonon states changes as the numbers m and n vary, and also the structure of the vibrational representations, which allows us to obtain information about the microstructure and perfection of these superlattices at the single-monolayer level by analyzing the Raman spectra.

1. INTRODUCTION

Interest in the investigation of first-order Raman scattering (RS) in semiconductor superlattices has continued to grow; this is because RS studies can yield a considerable volume of information not only about the quantization of various lattice vibrations but also about the nature of their interactions with the discrete quasi-two-dimensional excitons which are formed by localization of electron-hole pairs in the layers. It is obvious that the electron-phonon interaction in a quasi-two-dimensional electron gas can differ significantly from the three-dimensional case, not only in connection with the lowering of the dimensionality of the electronic system but also as a consequence of changes in the overall picture of the vibrational normal modes due to the superlattice.

Along with investigations of first-order RS,¹ there is much information to be gained by studying second-order RS in semiconductor superlattices, in which various combinations of two quantized lattice vibrations can participate in the scattering process. We know of only one paper² in which second-order RS is reported in a semiconductor superlattice; in this paper the authors investigated a GaAs–AlAs system with GaAs layer thicknesses $d_1 = 20 \text{ \AA}$ and AlAs layer thicknesses $d_2 = 60 \text{ \AA}$. The RS was excited with light quanta whose energies were nearly resonant with an exciton transition between the subbands of size-quantized ($n = 1$) heavy holes and electrons. Using the backscattering geometry from the (001) plane and parallel polarizations of the incident and scattered light, these authors observed several narrow lines caused by additive combinations of quantized GaAs LO_l phonons ($l = 2, 4, 6$).

In superlattices of A^3B^5 compounds the long-wavelength ($k \approx 0$) longitudinal LO_l phonons which propagate along the direction of quantization and which are trapped in the corresponding layers can be classified according to the irreducible representations (IR) of the point group D_{2d} , and have the symmetry $B_2(\Gamma_2)$ (for odd l) or $A_1(\Gamma_1)$ (for even l). When the first-order RS spectra are excited far from resonance with the electron transitions in the backscattering geometry from the (001) plane, phonons with Γ_2 symmetry are allowed when the incident and scattered light are cross-

polarized (xy), while phonons with Γ_1 symmetry are allowed when these polarizations are parallel (xx). In this notation the x -axis is directed along the [100] direction of the crystal, while the y -axis is along [010]. These selection rules are violated under resonance excitation conditions^{2,3} and phonons with Γ_2 symmetry are not experimentally observed.^{4–10}

In this paper we report the experimental observation of second-order RS in semiconductor $(\text{GaAs})_m(\text{AlAs})_n$ superlattices made up of size-quantizing heterostructures (the integers m and n are respectively the numbers of GaAs and AlAs layers in an elementary unit cell) under excitation far from resonance with the exciton transitions. In this work we have investigated scattering for both polarizations, parallel (xx) and crossed (xy), of the incident and scattered light, and also over a wide range of frequencies overlapping the region of additive combinations of LO_l phonons (for both even and odd l) which are trapped in both the GaAs and the AlAs layers.¹¹ Under these conditions we obtained the first-order RS spectra with high resolution: we observed sharp distinct lines corresponding to LO_l phonons with Γ_1 and Γ_2 symmetries trapped in a GaAs layer (up to $l = 11$) and in an AlAs layer (up to $l = 5$). We have carried out a comparison between the calculated LO_l phonon frequencies and measured frequencies obtained recently from experiments with scattering of slow neutrons in the case of bulk GaAs,¹⁰ and with perturbation-theory calculations which take into account the Coulomb interactions between ions in neighboring layers for the case of AlAs.¹²

In order to analyze the phonon symmetries and selection rules in second-order RS spectra, we have used the method of band representations (BR) of space groups,¹³ which is effective in studying crystals with a large number of atoms in a primitive unit cell. We establish that as the numbers of monolayers m and n change, the contributions of displacements of specific atoms to the phonon states changes as well as the structure of the vibrational representations, i.e., the phonon spectrum of the superlattices is significantly reconstructed. Thus, the approach developed here allows us to obtain useful information about the microstructure and perfection of the superlattice at the single-monolayer level

from analysis of the RS spectrum.

The most interesting part of this work is the investigation of second-order RS in superlattices. Because this scattering process takes place with the participation of overtone and mixing combinations of two phonons with equal and oppositely-directed wave vectors \mathbf{k}_1 and \mathbf{k}_2 ($\mathbf{k}_1 + \mathbf{k}_2 \approx 0$), corresponding to critical high-symmetry points of the phonon density-of-states function both at the center and at the edges of the Brillouin zone (BZ), the number of possible combinations of groups of atoms which contribute to these states is considerably increased. This in turn increases the analytical possibilities of second-order RS compared to first-order RS.

Our analysis allows us to obtain selection rules for the first time for second-order RS in this type of superlattice, which we use to interpret our experimental results.

2. EXPERIMENTAL TECHNIQUE AND BASIC SAMPLE CHARACTERISTICS

We investigated light scattering from two samples of semiconductor superlattice consisting of alternating ultrathin layers of the different semiconductors GaAs and AlAs, which have the same sphalerite crystal structure [space group $T_d^2(F43m)$] and nearly equal lattice constants [space group $T_d^2(F43m)$] and nearly equal lattice constants: $a_{\text{GaAs}} = 5.6533 \text{ \AA}$ and $a_{\text{AlAs}} = 5.6611 \text{ \AA}$.

The single-crystal samples of $(\text{GaAs})_m(\text{AlAs})_n$ semiconductor superlattice made up of size-quantizing heterostructure were grown by molecular-beam epitaxy on an n -type GaAs substrate oriented along the [001] axis. The layer thicknesses for samples 1 and 2 as determined from x-ray diffraction data were respectively

$$d_1 = 58.87 \text{ \AA} \quad (m=21) \text{ GaAs}, \quad d_2 = 18.05 \text{ \AA} \quad (n=6) \text{ AlAs};$$

$$d_1 = 20.75 \text{ \AA} \quad (m=7) \text{ GaAs}, \quad d_2 = 51.45 \text{ \AA} \quad (n=18) \text{ AlAs}.$$

Both samples had sharp and abrupt boundaries separating the heterolayers, with characteristic transition layer thicknesses $d_0 = 2.22 \text{ \AA}$ for sample 1 and $d_0 = 3.64 \text{ \AA}$ for sample 2. The period of the superlattices $d = d_1 + d_2$ in each sample was repeated 100 times. A typical sample size was $3 \times 5 \text{ mm}^2$. For comparison we also measured the RS spectra of single-crystal GaAs and AlAs samples of thickness 1–2 μm . These crystals were also grown by molecular-beam epitaxy on n -type GaAs substrates oriented along the [001] axis.

The RS spectra were excited by radiation from a CW argon laser with wavelength 4880 and 5145 \AA . The geometry used was backscattering along the quantization (growth) axis $z \parallel [001]$; $z(xx)\bar{z}$ for parallel, $z(xy)\bar{z}$ for crossed polarizations of the incident and scattered light. The x and y axes were parallel to the [100] and [010] axes, respectively. The samples were bonded with silver paste to the cold finger of a helium pumped metallic cryostat, providing a temperature from 1.2 to 300 K. The scattered light was analyzed with a triple diffraction monochromator using an RCA 31034A cooled photomultiplier in the photon-counting regime.

3. EXPERIMENTAL RESULTS AND DISCUSSION

a. Analysis of the first-order spectra

We will begin our discussion of RS by quantized optical phonons with first-order RS, and then proceed to second-order RS.

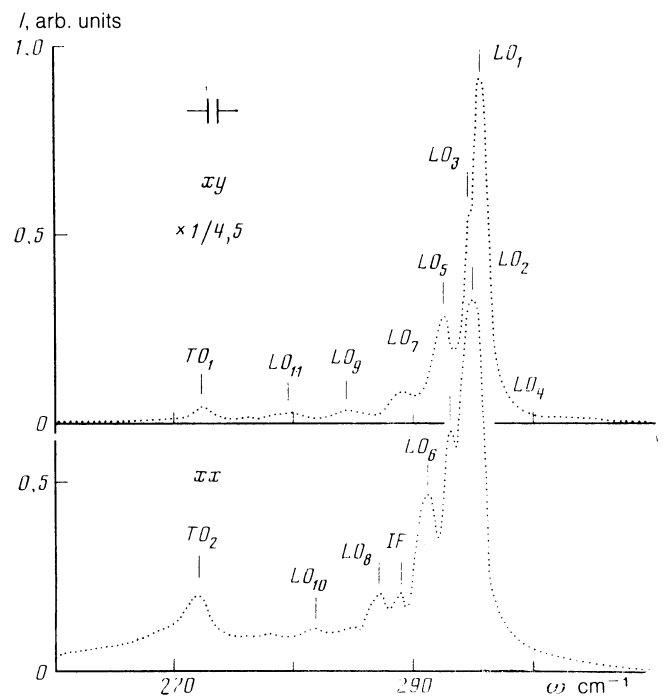


FIG. 1. First-order RS spectra of LO_i phonons trapped in GaAs layers of the superlattices $(\text{GaAs})_{21}(\text{AlAs})_6$ in the crossed (xy) and parallel (xx) scattering geometries. $T = 10 \text{ K}$, $\hbar\omega_i = 2.409 \text{ eV}$.

In Fig. 1 we present typical first-order RS spectra in $(\text{GaAs})_{21}(\text{AlAs})_6$ superlattices obtained using the crossed (xy) and parallel (xx) scattering geometries at a temperature $T = 10 \text{ K}$ in the vicinity of the longitudinal optical phonon frequencies for gallium arsenide. The wavelength of the laser radiation equalled 5145 \AA , i.e., the energy of the excitation radiation quanta $\hbar\omega_i = 2.409 \text{ eV}$ was far from the strongest of the exciton transition resonances, which were present in these samples in the energy range 1.62 to 2.05 eV. Analogous spectra were also obtained for excitation at the wavelength 4880 \AA . Thus, all the features shown in Fig. 1 are caused by light scattering and not hot-carrier luminescence.

For comparison we have measured the frequency of long-wavelength $LO(\Gamma)$ phonons in the spectra of bulk samples of GaAs and AlAs (also grown by molecular-beam epitaxy). These spectra were obtained under the same experimental conditions, i.e., the scattering geometry, width of the gaps, temperature, etc. The measured values of the frequencies came to 296.0 and 405.8 cm^{-1} for GaAs and AlAs, respectively. The presence of a series of sharp distinct lines in the spectra of $(\text{GaAs})_{21}(\text{AlAs})_6$ at frequencies below the above-mentioned values of the $LO(\Gamma)$ phonon frequencies of the bulk samples is caused by the appearance of size-quantized optical phonons in the superlattices.

Strictly speaking, the phonon spectrum of a superlattice cannot be obtained from the spectra of bulk GaAs and AlAs by viewing it as the spectrum of a system with a superimposed perturbation (since in the transition to the superlattice the number and type of atoms in a primitive cell also changes); nevertheless the vibrations of the superlattice can be placed in one-to-one correspondence with the vibrations of the bulk crystal by subdividing the BZ. The presence of a new periodicity in superlattices with size-quantizing heterostructure leads to the formation of mini-Brillouin zones,

which result in subdivision of the phonon dispersion curves $\nu(\mathbf{k})$ of the bulk crystal.

Because there is a mismatch between the dispersion curves of the original crystals of GaAs and AlAs, the effects of quantization on the acoustic and optical phonons are quite different. Thus, the bulk dispersion curves of acoustic phonons, and consequently the acoustic phonon densities of states, overlap over a wide range of frequencies for the original layers of GaAs and AlAs; therefore superlattice acoustic phonons can be well extended in both layers. In contrast, the dispersion curves of optical phonons do not overlap; therefore the mismatched phonons will be evanescent, and the superlattice modes are found to be trapped in the original layers with properties typical of standing waves. In $(\text{GaAs})_m(\text{AlAs})_n$ superlattices the frequencies of the optical phonons trapped in the GaAs (or AlAs) layers correspond to the frequencies of those phonons in bulk crystals of GaAs (or AlAs) whose wave vectors, taking into account boundary conditions on the amplitudes of oscillation in the approximation of infinitely small decay length, are determined by the following relations¹⁴⁻¹⁵:

$$k_l^{\text{GaAs(AlAs)}} = l\pi [m(n) + 1] d_0, \quad (1)$$

where l , the order of the trapped phonon, takes on integer values $1 \leq l \leq m(n)$, and d_0 , the thickness of monolayers of GaAs and AlAs, equals 2.83 \AA . Under conditions of complete trapping, l equals the number of half-waves of the sinusoidal wave function of the trapped mode confined in the GaAs and AlAs layers. Note that this relation differs somewhat from the equations which describe the formation of standing waves in thin isolated dielectric films, for which 1 does not appear in the square brackets. In superlattices with alternating layers, because they decay lengths of the vibrations take on finite values, the factor in the square brackets can take on values intermediate between $m(n)$ and $m(n) + 1$. The high optical quality of the samples we studied, the perfection of their structure, and the optimization of the measurement regime, allow us to observing scattering of light up to order $l = 11$ for trapping in the GaAs layer and to $l = 5$ in the AlAs layers.

As we have already noted, when the trapped modes are optical phonons, the active phonons appearing in the first-order RS spectra have symmetry Γ_1 (even l) in the (xx) geometry, while those which are active in the (xy) geometry have symmetry Γ_2 (odd l). The measured values of frequencies of longitudinal trapped phonons are presented in Table I. In this same table we list calculated values obtained from a model of a two-atom linear chain in the effective-mass ap-

proximation.⁵⁻⁷ It is clear that agreement between experimental and calculated data is good. The measured values of the frequencies of LO_l -phonons trapped in the AlAs layers¹⁷ equal $404.1, 401.9, 399.4, 395.2,$ and 389.4 cm^{-1} for $l = 1-5$ respectively, which agrees well with the theoretical data on the dispersion of LO_l phonons in bulk AlAs (Ref. 18) (for $k = 0, \omega_{LO(r)} = 405.8 \text{ cm}^{-1}$); this data was obtained in Ref. 12 using perturbation theory in an adiabatic model of the bound charge, taking into account the Coulomb interactions between ions in neighboring layers.

b. Analysis of the phonon spectrum of superlattices using the method of band representations of space groups

The symmetries of superlattices as a function of the number of mono-layers $(m + n)$ in a primitive cell are described by two different space groups: D_{2d} (for $m + n = 2k$) and $D_{2d'}$ (for $m + n = 2k + 1$).¹⁹ Earlier work on RS in superlattices was limited to investigating the point group D_{2d} as a basis for symmetry analysis of the superlattice phonons¹, i.e., to phonons with $\mathbf{k} = 0$. In this paper we will use the space group band representation (BR) method to classify the symmetries of superlattice phonons with nonzero values of wave vector.¹³

Band representations of space groups establish the connection between local properties of a system (in the problem under discussion here the local atomic displacements) and its band characteristics (the normal vibrations of the crystal lattice). From the point of view of group theory, a Br is a reducible representation of the infinite-dimensional space group constructed by joining the irreducible representations of the space group at all points in the Brillouin zone. It can be characterized by assigning sets of irreducible representations only at inequivalent symmetry points of the BZ, and at one point of each of the inequivalent symmetry elements of the BZ (lines or planes); at the remaining points of the BZ these IRs are obtained from the compatibility relations.

Superlattices constitute ideal model systems in that they allow us to demonstrate all the possible uses of the BR method for analyzing the symmetries of phonons in crystals. From the point of view of symmetry, superlattices with different m and n are different crystals; they differ even in the limit of a single space group for the crystalline microstructure, i.e., in the placement of atoms in the unit cell at symmetry positions (i.e., the Wyckoff positions).

Analyses of the phonon symmetries which employ the usual method of constructing the full vibrational representation and then resolving the factor group of the crystal in terms of IRs (known as the Bhagavantam-Venkatarayudu

TABLE I. Comparison of measured values of the LO_l phonons ($\omega_{LO_l}^{\text{exp}}$) trapped in GaAs layers in the superlattice $(\text{GaAs})_{21}(\text{AlAs})_6$ with calculated values ($\omega_{LO_l}^{\text{calc}}$) obtained in a model of a two-atom linear chain.

Phonon trapping order and symmetry		$\omega_{LO_l}^{\text{exp}}, \text{cm}^{-1}$	$\omega_{LO_l}^{\text{calc}}, \text{cm}^{-1}$	Phonon trapping order and symmetry		$\omega_{LO_l}^{\text{exp}}, \text{cm}^{-1}$	$\omega_{LO_l}^{\text{calc}}, \text{cm}^{-1}$
Γ_2	Γ_1			Γ_2	Γ_1		
1	—	295.7	295.82	7	—	288.5	288.40
—	2	295.1	295.30	—	8	285.7	285.81
3	—	294.4	294.45	9	—	284.0	283.39
—	4	293.3	293.27	—	10	281.6	281.61
5	—	292.2	291.80	11	—	279.0	278.80
—	6	290.6	290.05				

method)²⁰, or the method of positional symmetry described in Ref. 21, do not allow this problem to be solved in its general form for arbitrary m and n . Consequently, there are certain overall regularities which these methods cannot reveal; rather, they require us to recalculate everything for each specific structure. Furthermore, the general method of constructing vibrational representations is very cumbersome, especially for a crystal with a larger number of atoms in its primitive cell, as is the case for superlattices. Although the method of positional symmetry is simpler, it is nevertheless quite complex, especially for phonons with $\mathbf{k} \neq 0$.

In the approach we adopt here it is enough to construct the BR for at most two space groups D_{2d}^5 and D_{2d}^9 , and then to find the general expressions for the placement of the atoms according to the Wyckoff positions. This information turns out to be enough to carry out the symmetry analysis of the phonon spectrum of any of the superlattices under discussion here.

We have determined that there exist eight inequivalent types of placement of atoms according to the Wyckoff positions, corresponding to different combinations of the numbers m and n , and we have constructed the BR of the space groups in question,²² which coincide with what was presented in Ref. 23. The analysis we give here shows that the symmetry types of the phonons for all superlattices with the same symmetry group are independent of the specific values of m and n . However, the contribution of the displacements of specific atoms to the phonon states depends on the number of layers, because in varying the number of layers we change the placement of atoms according to the Wyckoff positions. In this case the structure of the vibrational representation also changes, i.e., the number of phonon branches with a given symmetry. Below we will apply these results to analysis of experiments for specific values of m and n .

The symmetry of the superlattices $(\text{GaAs})_{21}(\text{AlAs})_6$ ($m + n = 27$) is described by the space group D_{2d}^9 . An elementary unit cell contains 54 atoms; the number of vibrational branches in such a system is 162. The placement of the atoms according to their Wyckoff positions (see Fig. 2) is as follows: one Ga atom is located at the position $1a(000)$ with local symmetry $42m$, one As atom is at position $1c(0\frac{1}{2}\frac{1}{2})$ with local symmetry $42m$, 20 Ga atoms and 6 Al atoms are pairwise located at $2e(00z)$ ($00\bar{z}$) with local symmetry mm , and 26 As atoms are in the positions $2f(0\frac{1}{2}z)$ ($10\bar{z}$) with local symmetry mm .

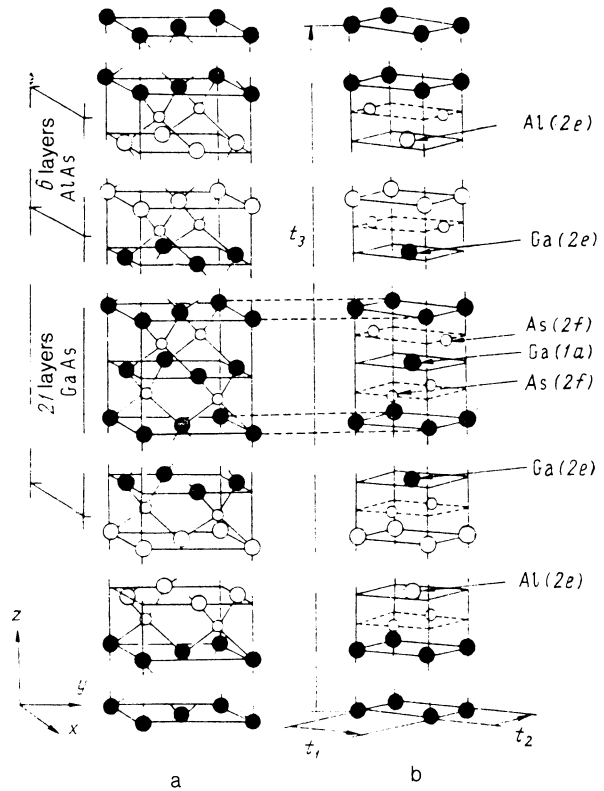


FIG. 2. Crystal structure of $(\text{GaAs})_{21}(\text{AlAs})_6$ superlattice and placement of atoms according to the Wyckoff positions: a—cubic and b—centered tetragonal unit cells.

The symmetries of the phonons in this system are shown in Table II. In the first column we list the designations of the Wyckoff positions according to Ref. 24, with an indication of what atoms occupy them, the coordinates of these positions in units of the vectors of the basic translations for doubling the primitive cell (t_1, t_2, t_3), and their local symmetry groups. In the second column we list those IRs of the local group according to which the components of the vectors of the local atomic displacements transform (the notation of the IRs is given as in Ref. 23). The third and subsequent columns contain the BZ labels in the k -basis obtained by inducing the local group with the corresponding IR, i.e., the labels of the IR of the group of the wave vector which are unambiguously connected with the IR of the whole space

TABLE II. Symmetry of the phonons in a $(\text{GaAs})_{21}(\text{AlAs})_6$ superlattice.

D_{2d}^9	Γ	M	X	P	N
$2d \bar{4} m 2$	$(000) \bar{4} 2m$	$(\frac{1}{2} \frac{1}{2} \frac{1}{2}) \bar{4} 2m$	$(00 \frac{1}{2}) 222$	$(\frac{1}{4} \frac{1}{4} \frac{1}{4}) \bar{4}$	$(0\frac{1}{2}0) m$
$1\text{Ga}(a)(000) \bar{4} 2m$	$b_2(z)$ $e(x, y)$	$\frac{2}{5}$	$\frac{2}{3.4}$	$\frac{2}{3.4}$	$\frac{1}{1.2}$
$1\text{As}(c)(0\frac{1}{2}\frac{1}{2}) \bar{4} 2m$	$b_2(z)$ $e(x, y)$	$\frac{2}{5}$	$\frac{4}{1.2}$	$\frac{4}{1.2}$	$\frac{1}{1.2}$
$10 \times 2\text{Ga}(e)$ $3 \times 2\text{Al}(e)$ $(00z)(00\bar{z}) mm$	$a_1(z)$ $b_1(x)$ $b_2(y)$	$\frac{1.2}{5}$ $\frac{5}{5}$ $\frac{5}{5}$	$\frac{1.2}{5}$ $\frac{3.4}{3.4}$ $\frac{3.4}{3.4}$	$\frac{1.2}{3.4}$ $\frac{3.4}{3.4}$ $\frac{3.4}{3.4}$	$\frac{1.1}{1.2}$ $\frac{1.2}{1.2}$ $\frac{1.2}{1.2}$
$13 \times 2\text{As}(f)$ $(0\frac{1}{2}z)$ $(\frac{1}{2}0\bar{z}) mm$	$a_1(z)$ $b_1(x)$ $b_2(y)$	$\frac{1.2}{5}$ $\frac{5}{5}$ $\frac{5}{5}$	$\frac{1.2}{5}$ $\frac{1.2}{1.2}$ $\frac{1.2}{1.2}$	$\frac{3.4}{1.2}$ $\frac{1.2}{1.2}$ $\frac{1.2}{1.2}$	$\frac{1.1}{1.2}$ $\frac{1.2}{1.2}$ $\frac{1.2}{1.2}$

group and which determine the symmetry of the phonons at the corresponding symmetry points of the BZ. The symbol of the symmetry point of the BZ, its coordinate in units of the reciprocal lattice vectors and the corresponding point group of the wave vector are shown in the legend of each column. (For IRs of the groups of the wave vector we use the notation adopted in Ref. 25.)

Once we have analyzed Table II, we can easily convince ourselves that phonons of a definite symmetry are associated with vibrations of a specific group of atoms. For example, the vibrational representation at the Γ point has the form

$$26\Gamma_1(\text{Ga}_{a,z}; \text{Al}_{e,z}; \text{As}_{f,z}) + 28\Gamma_2(\text{Ga}_{a,z}; \text{Al}_{e,z}; \text{As}_{c,z}) + 54\Gamma_3(\text{Ga}_{a,xy}; \text{Al}_{e,xy}; \text{As}_{c,f}), \quad (2)$$

where the upper indices of the element symbols denote the components of atomic displacement, while the lower indices are the Wyckoff positions in which those atoms are found which give contributions to the vibrations with the given symmetry. From this expression it is clear that only the z-displacements of the Ga and Al atoms found in the e positions and the As atoms in the f positions contribute to the vibrations with symmetry Γ_1 , while the Ga atom in the a position and the As atom in the c position give no contribution. Analysis of phonon symmetries from other symmetry points of the BZ whose combinations can appear in the second-order RS spectra significantly increase the number of possible variants. This allows us to obtain a wealth of information about the superlattice microstructure.

In order to analyze the second-order RS spectra we have determined the selection rules for those phonon combinations which are active in scattering; the symmetries of these phonons are given in Table II. First of all, we determined the critical points of the phonon density of states functions for vibrations of various symmetries, and established that the Γ -point is critical for vibrations Γ_1 and Γ_2 , M is critical for M_1 and M_2 , and P is critical for P_1 and P_2 .

We then determined that the following combinations of phonons were involved in the scattering for second-order RS spectra in the (xx) geometry:

$$\Gamma_1 \times \Gamma_1, \Gamma_2 \times \Gamma_2; M_1 \times M_1, M_2 \times M_2; P_1 \times P_1, P_2 \times P_2, P_1 \times P_2,$$

while for the (xy) geometry,

$$\Gamma_1 \times \Gamma_2; M_1 \times M_2; P_1 \times P_2.$$

c. Analysis of the second-order spectra

Typical light scattering spectra in the frequency region corresponding to second-order scattering for the superlattices $(\text{GaAs})_{21}(\text{AlAs})_6$ are presented in Fig. 3. These spec-

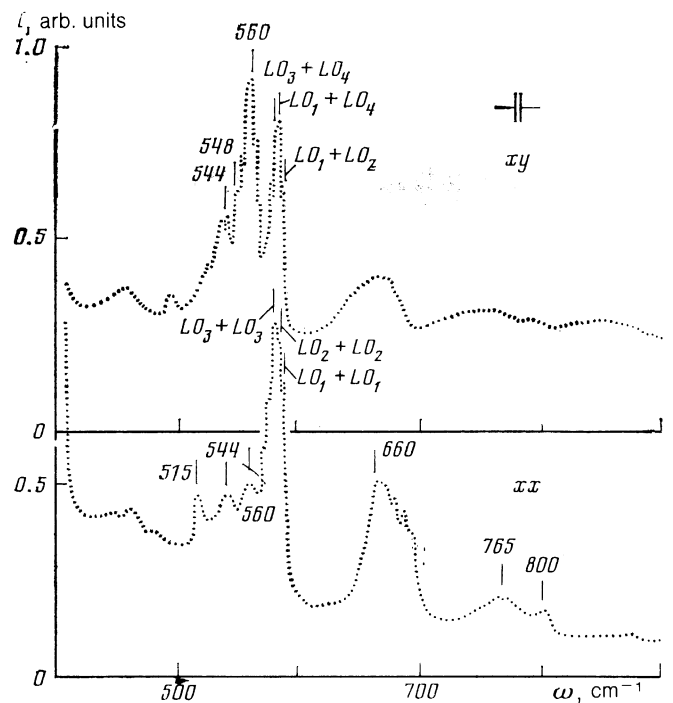


FIG. 3. Second-order RS spectra of $(\text{GaAs})_{21} \cdot (\text{AlAs})_6$ superlattice in crossed (xy) and parallel (xx) geometries of scattering. $T = 10$ K, $\hbar\omega_i = 2.409$ eV.

tra were obtained by laser excitation in the (xx) and (xy) scattering geometries, where the laser wavelength was 5145 \AA . In both polarizations we observed sharp distinct lines which can be grouped in the following way: in the frequency region $550\text{--}600 \text{ cm}^{-1}$ the lines are caused by various additive combinations of optical phonons trapped in the GaAs layers. The wide band in the region frequencies $650\text{--}700 \text{ cm}^{-1}$ is apparently due to additive combinations of vibrations associated with the boundaries. The frequency region $750\text{--}820 \text{ cm}^{-1}$ corresponds to additive combinations of optical phonons trapped in the AlAs layers.

In analyzing the second-order RS spectra for $(\text{GaAs})_m(\text{AlAs})_n$ superlattices we must take into account the following fact: when we measured the spectra of bulk GaAs under the same conditions as our superlattice measurements, i.e., $T = 10$ K, with $\hbar\omega_i = 2.409$ eV far from any exciton resonances, we observed a frequency shift of the $2LO(\Gamma)$ phonon $\omega_{2LO(\Gamma)} = (584 \pm 1) \text{ cm}^{-1}$, which is $(8 \pm 1) \text{ cm}^{-1}$ less than the doubled value of the $LO(\Gamma)$ phonon frequency $\omega_{LO(\Gamma)} = (296 \pm 1) \text{ cm}^{-1}$. An analogous situation obtains when we compare the spectra of

TABLE III. Identification and frequencies of LO_i phonons trapped in GaAs layers in the second-order RS spectra of $(\text{GaAs})_{21}(\text{AlAs})_6$ superlattices.

Geometry of scattering			
xx		xy	
Phonon combination	Frequency, cm^{-1}	Phonon combination	Frequency, cm^{-1}
$LO_1+LO_1(\Gamma_2 \times \Gamma_2)$	591.4	$LO_1+LO_2(\Gamma_1 \times \Gamma_2)$	586.3
$LO_2+LO_2(\Gamma_1 \times \Gamma_1)$	590.2	$LO_1+LO_4(\Gamma_1 \times \Gamma_2)$	582.4
$LO_3+LO_3(\Gamma_2 \times \Gamma_2)$	588.8	$LO_3+LO_4(\Gamma_1 \times \Gamma_2)$	580.5

$2LO(\Gamma)$ phonons excited by light which is resonant with the gap $E_0 + \Delta_0 \approx 1.85$ eV (where E_0 is the width of the GaAs band gap and Δ_0 is the spin-orbit splitting), i.e., also far from any exciton resonances.² This shift can be explained, in particular, by the fact that for two-phonon scattering real transitions can occur between parabolic states of the conduction and valence bands with the emission of an $LO(\Gamma)$ phonon. As the energy of the quanta of the excitation radiation increases, $LO(\Gamma)$ phonons with large wave vectors become involved in the scattering process in order to sustain these real transitions; it follows from the dispersion relations for GaAs that these phonons have low frequency.

We anticipate that the analogous situation can also take place for the case of RS in the superlattices $(\text{GaAs})_m(\text{AlAs})_n$. Then in order to interpret the second-order RS spectra shown in Fig. 3 it is necessary to include relative displacements of the lines corresponding to RS of two trapped LO_l phonons; these displacements are roughly $(8 \pm 1) \text{ cm}^{-1}$ lower in frequency than the corresponding values obtained from the first-order RS spectra.

Taking into account what was said in connection with the selection rules we have obtained for second-order RS, and the analysis of the dispersion curves and the first- and second-order RS spectra for bulk gallium arsenide carried out in Refs. 10, 18 (which were obtained under the same conditions), we offer possible interpretations for the most intense lines in the second-order RS spectrum of the superlattice $(\text{GaAs})_{21}(\text{AlAs})_6$ in Table III.

Our experimental investigation of first- and second-order RS in semiconductor superlattices and subsequent analysis using the space group BR method are interesting with regard to general physics from the point of view of possible use of single-crystal superlattices as felicitous model objects for a variety of applications of the BR method itself. Furthermore, these concurrent experimental and theoretical investigations allow us to obtain a wealth of information about the microstructure of superlattices and open up new possibilities for RS spectroscopy of superlattices.

The authors acknowledge their debt to B. P. Zakharchen and I. P. Ipatova for useful discussions of the work.

¹University of Illinois, Champaign-Urbana, USA.

- ¹M. V. Klein, IEEE J. Quant. Electr. **QE-22**, 1760 (1986).
²A. K. Sood, J. Menendez, M. Cardona, and K. Ploog, Phys. Rev. B **32**, 1412 (1985).
³A. K. Sood, J. Menendez, M. Cardona, and K. Ploog, Phys. Rev. Lett. **54**, 2111 (1985).
⁴K. Kubota, M. Nakayama, H. Katoh, and N. Sano, Solid State Commun. **49**, 157 (1984).
⁵C. Colvard, T. Gant, M. V. Klein *et al.*, Phys. Rev. B **31**, 2080 (1985).
⁶B. Jusserand, D. Paquet, and A. Regnery, *Superlattices and Microstructures* **1**, 61 (1985).
⁷B. Jusserand, D. Paquet, and A. Regnery, Phys. Rev. B **30**, 6245 (1984).
⁸A. Ishibashi, M. Itabashi, Y. Mori *et al.*, Phys. Rev. B **33**, 2887 (1986).
⁹A. C. Maciel, L. C. C. Cruz, and J. F. Ryan, J. Phys. C **20**, 3041 (1987).
¹⁰E. Richter and D. Strauch, Solid State Commun. **64**, 867 (1987).
¹¹B. H. Bairamov, R. A. Evarestov, I. P. Ipatova *et al.*, Booklet of Abstracts, 4th Int. Conf. Superlattices, Microstructures and Microdevices, Miramare, Trieste, 1988, p. 56.
¹²S. K. Yip and Y. C. Chang, Phys. Rev. B **30**, 7037 (1984).
¹³R. A. Evarestov and V. P. Smirnov, *Metody teorii grupp v kvantovoi khimii tverdogo tela (Group-Theoretic Methods in Solid-State Quantum Chemistry)*. Leningrad: Izd. LGU, 1987.
¹⁴E. Molinari, A. Fasolino, and K. Kunc, Phys. Rev. Lett. **56**, 1751 (1986).
¹⁵B. Jusserand and D. Paquet, Phys. Rev. Lett. **56**, 1752 (1986).
¹⁶A. K. Sood, J. Menendez, M. Cardona, and K. Ploog, Phys. Rev. Lett. **56**, 1753 (1986).
¹⁷B. Kh Bairamov, Preprint No. 1192, Physico-Technical Institute (1987).
¹⁸G. Dolling and J. L. T. Waugh, *Lattice Dynamics*, R. F. Wallis ed. (Pergamon, London, 1965), p. 19.
¹⁹J. Sapriel, J. C. Michel, J. C. Tolédano *et al.*, Phys. Rev. B **28**, 2007 (1983).
²⁰S. Bhagavantam and T. Venkatarayudu, *Theory of Groups and its Application to Physical Problems*, Academic, New York (1969).
²¹G. N. Zhizhin, B. N. Mavrin, and V. F. Shabanov, *Opticheskiye kolebatel'nye spektry kristallov (Optical Phonon Spectra of Crystals)*. Moscow, Nauka, 1984.
²²Yu. E. Kitaev and R. A. Evarestov, Fiz. Tverd. Tela (Leningrad) **30**, 2970 (1988) [Sov. Phys. Solid State **30**, 171L (1989)].
²³O. V. Kovalev, *Neprirodime i inducirovannye predstavleniya i kopredstavleniya fedorovskikh grupp (Irreducible and Induced Representations and Corepresentations of Fedorov Groups)*. Moscow, Nauka, 1986.
²⁴*International Tables for Crystallography*, Theo Hahn ed., Vol. A: Space-Group Symmetry (Dordrecht-Boston, Reidel, 1983).
²⁵S. C. Miller and W. F. Love, *Tables of Irreducible Representations of Space Groups and Corepresentations of Magnetic Space Groups*, Boulder, Colorado, 1967.

Translated by Frank J. Crowne